Dechanneling of MeV protons by 60° dislocations

M. B. H. Breese and P. J. C. King
Scanning Proton Microprobe Unit, Nuclear Physics Laboratory, University of Oxford, Keble Road, Oxford, OX1 3RH, United Kingdom

P. J. M. Smulders
Nuclear Solid State Physics, Materials Science Centre, Groningen University, Nijenborgh 4, 9747 AG Groningen, The Netherlands

G. W. Grime
Scanning Proton Microprobe Unit, Nuclear Physics Laboratory, University of Oxford, Keble Road, Oxford OX1 3RH, United Kingdom
(Received 26 July 1994)

This paper describes a model for interpreting experimental transmission ion channeling results for dechanneling by 60° misfit dislocations in epitaxial $Si_{1-x}Ge_x/Si$ material in terms of rotated lattice planes of the $Si_{1-x}Ge_x$ epilayer with respect to the silicon substrate. A Monte Carlo channeling simulation program is used to model the trajectories of the incident MeV protons through the epilayer and the thinned Si substrate in order to calculate the average transmitted proton energy as a function of the sample-tilt angle about the beam axis and the effective rotation angle of the epilayer. The conditions under which the 60° dislocations can be resolved from the surrounding perfect crystal and also resolved from adjacent 60° dislocations causing a slightly different amount of lattice plane rotation are discussed using this model. Good agreement is demonstrated with experimental results showing the variation in transmitted proton energy across a group of five 60° dislocations for different sample-tilt angles.

I. INTRODUCTION

There is current interest in growing epitaxial strained layer systems of lattice mismatched semiconductors, such as $Si_{1-x}Ge_x/Si$, in order to alter the energy band gap and hence the electronic properties of the material.[1] If there is too much strain present in a growing lattice-mismatched epitaxial layer, it is relieved by the formation of misfit dislocations[2] which degrade the electronic properties of the material. When MeV ions are aligned with a crystal axis or plane, their trajectories are sensitive to any disruption of the perfect lattice, and this effect can be used to characterize the crystalline properties of the material.[3] There has been considerable effort in measuring both the amount of strain present in epitaxial lattice-mismatched semiconductor layers using channeled MeV ions[4–8] and also characterizing the interaction of MeV ions with different types of dislocations[3,4,8–10] in order to determine their depth distribution and concentration.

This paper characterizes the dechanneling effects of 60° misfit dislocations on the trajectories of MeV protons transmitted through epitaxial $Si_{1-x}Ge_x/Si$ materials. In order to distinguish between dechanneling from dislocations and strain-induced dechanneling, only channeling along the surface-normal growth direction is considered, so that strain-induced dechanneling is not present. The main dechanneling mechanism of 60° dislocations is first discussed, and then it is described how this can be simulated using a Monte Carlo method based on rotated planes of the epilayer with respect to the substrate. These simulated results for MeV protons dechanneling from 60° dislocations are then compared with experimental results measured with a nuclear microprobe, showing the variation in the transmitted proton energy across spatially resolved bunches of 60° dislocations in $Si_{1-x}Ge_x/Si$.

II. DECHANNELING

A. Previous work on dechanneling from dislocations

Ions which are incident along a major crystal axis or plane have a channeled trajectory, resulting in a lower rate of energy loss and a lower nuclear encounter probability than ions which are incident along a nonchanneled trajectory. This is because the ions are steered into regions of lower electron density between the channel walls. The critical angle ψ_c is the maximum angle for which channeling will take place when an ion is incident in the center of a channel.[3] At larger angles between the incident beam and the channel walls, the average rate of energy loss increases since the channeling planes cannot provide the repulsive force necessary to steer the ions back into the channel. The variation of the measured backscattered ion yield as a function of tilt angle about a channeling direction is characterized using a different definition. The measured angular half-width of the channeling dip is denoted as $\psi_{1/2}$. The different between ψ_c and $\psi_{1/2}$ is usually less than 20%.[3]

The plane rotation associated with dislocations can result in initially well-channeled ions being dechanneled. For 90° dislocations and 0° dislocations, the plane rotation is large at the dislocation core and decreases away from it, such that the dechanneling effect decreases away from the core. These types of dislocations have been characterized by a dechanneling factor σ. This was defined as the diameter of a region around the dislocation line in which dechanneling occurs, and it is inversely pro-

 ©1995 The American Physical Society

portional to the channeling critical angle.[3,10] MeV α particles typically have a dechanneling factor in silicon of $\sigma \approx 3$ nm in axial alignment ($\psi_c \approx 0.8°$) and $\sigma \approx 20$ nm in planar alignment ($\psi_c \approx 0.2°$). The measured rise in the backscattered ion yield with depth in channeled alignment has been used to deduce the depth distribution of dislocations present.[3,4,8,9] A little work has been carried out[11] on characterizing the dechanneling effect of 60° dislocations, but they have mainly been treated as resulting in a similar dechanneling effect as 90° dislocations.

It has been previously demonstrated how bunches of 60° misfit dislocations in epitaxial $Si_{0.85}Ge_{0.15}/Si$ (Refs. 12 and 13) and single 60° misfit dislocations in $Si_{0.95}Ge_{0.05}/Si$ (Ref. 14) could be resolved in transmission channeling images using the Oxford nuclear microprobe[15] with a 2–3-MeV proton beam focused to a spot size of about 200 nm. For this method the $Si_{1-x}Ge_x/Si$ crystal sample was thinned from the rear to about 20 μm and the average transmitted energy of MeV protons was measured as a function of focused beam position within the scanned area, with the substrate [001] axis aligned with the incident beam. Channeled ions lose energy at a lower rate than nonchanneled ions.[16,17] The measured transmitted proton energy at dislocations was therefore lower than that from the surrounding perfect crystal with the sample in channeled alignment because the 60° dislocations dechanneled some of the ions, which subsequently traveled through the substrate with a high rate of energy loss. MeV protons, which have a narrower critical angle than MeV α particles, were used for this work. Their dechanneling factor is larger, and so protons farther away from the dislocation core are dechanneled, resulting in a more detectable signal. The use of MeV protons also enables thicker samples to be used because of their longer range. Transmission ion channeling has the advantage over transmission electron microscopy (TEM) in that it can analyze samples that are tens of micrometers in thickness. This significantly reduces sample preparation time compared with TEM and enables large areas of the sample to be analyzed. X-ray topography can be applied to bulk samples, but has a poorer spatial resolution than transmission ion channeling, which thus falls somewhere between these two established techniques in its capabilities.

Previous work has only characterized the dechanneling effects of dislocations when the incident ions are aligned with a planar or axial channel. The effect of tilting the sample slightly away from alignment was not previously considered since the measured channeling information would be integrated over a large number of dislocations with different magnitudes and signs of the rotation angle. The use of a nuclear microprobe enables dislocations to be spatially resolved, and so the effects of tilting the sample on channeling at the dislocations can be distinguished from the effects in the surrounding crystal. This advance in the experimental capability of ion channeling to spatially resolve dislocations enables the calculated variation of dechanneling across bunches of 60° dislocations to be compared here with experimental results on two $Si_{1-x}Ge_x/Si$ materials, where the surface-normal direction is the [001] axis.

B. Dechanneling effects of 60° dislocations

For all four possible 60° dislocation geometries, the Burgers vector can be resolved into components which are either edge or screw in character. For example, a dislocation with a Burgers vector of $(a/2)$ [101] can be resolved into components $(a/4)[1\bar{1}0]$, $(a/4)$[110], and $(a/2)$[001], where a is the lattice parameter of silicon, equal to 0.543 nm. If this dislocation has a line direction along $[1\bar{1}0]$, the $(a/4)[1\bar{1}0]$ corresponds to a screw component, $(a/4)$[110] corresponds to an edge component, and $(a/2)$[001] corresponds to an edge component with a Burgers vector perpendicular to the interface. Only the $(a/4)[1\bar{1}0]$ component relieves lattice mismatch. If only the $(a/2)$[001] component, which is the largest, is considered, the adjacent $[1\bar{1}0]$ dislocations in a bunch comprise a low-angle boundary, as shown in Fig. 1.[12] The (001) planes in the epilayer close to the interface are on average rotated through an angle δ about the $[1\bar{1}0]$ axis, and as a result, the (110) planes close to the interface are rotated by approximately the same amount. If adjacent 60° dislocations have edge components $(a/2)$[001] of the same sign, then the (110) planes are all rotated in the same sense and can be thought of as a dislocation bunch. For some bunches the (110) planes near to the interface are rotated in the sense shown in Fig. 1, while for other bunches the planes are rotated in the opposite sense with respect to the [001] substrate. The approximate angle through which the planes are rotated can be calculated from $\delta = b/l$, where $b = a/2$ is the length of the $(a/2)$[001] component of the Burgers vector and l is the average dislocation spacing. This consideration of the dechanneling effect of 60° dislocations in terms of the $(a/2)$[001] component was previously used to qualitatively explain the observed changes in contrast in transmission ion channeling images[12,13] at different sample-tilt angles with respect to the substrate [001] axis. Monte Carlo channeling simulations described here were not then available, and so this paper is an advance on this previous experimental work by considering under what

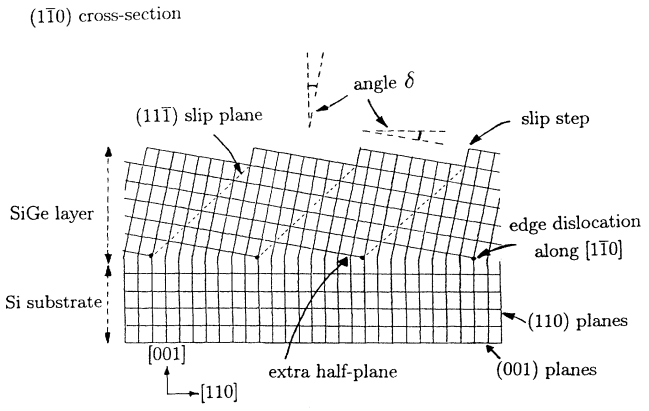

FIG. 1. $(1\bar{1}0)$ cross-sectional diagram showing how a series of edge dislocations along $[1\bar{1}0]$ with their Burgers vector $(a/2)$[001] all in the same sense form a low-angle boundary rotating the (110) planes in the epilayer through an angle δ.

tilt angle conditions the 60° dislocations can be resolved from the surrounding perfect crystal and also from adjacent bunches of 60° dislocations. It is also shown how plane rotation angles associates with 60° dislocations can be determined.

III. SIMULATION OF DECHANNELING FROM 60° DISLOCATIONS

To perform a rigorous calculation of the dechanneling effect of 60° misfit dislocations present at the interface between the substrate and epilayer, the resultant displacements of all the atoms both above and below the interface should be calculated and then the trajectory of the incident protons simulated through this system. However, the resultant displacements of the atoms in the substrate are difficult to accurately characterize and this procedure would also obscure the more general conclusions about the dechanneling mechanism of 60° dislocations. The simplifying assumption is made here that dechanneling mainly arises from the extra half planes of the $(a/2)[001]$ component inserted at the interface, which causes plane rotation of the overlying epilayer through an angle δ with respect to the [001] substrate. It is assumed that the plane rotation is a maximum at the core of the bunches of dislocations, and it relaxes with increasing lateral distance away from the core toward alignment with the planes of the substrate, so that the plane rotation angles varies in magnitude across the bunch, but the sign is the same in any one bunch.

In the Monte Carlo computer simulations, the regions on both sides of the boundary were assumed to be an ideal, undistorted Si crystal. The orientation of the top layer with respect to the bulk is given by a rotation δ about the $[1\bar{1}0]$ axis, lying in the boundary plane, as shown in Figs. 1 and 2. For each combination of δ and the tilt angle θ of the sample as a whole with respect to the proton beam, a total of 3600 ion trajectories were simulated, and the average energy after transmission through the bylayer was determined. An adapted version of the program FLUX3 was used,[18,19] which utilizes a

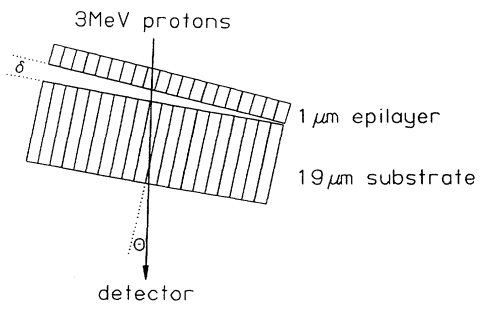

FIG. 2. Schematic of the geometry used to simulate the effects of 60° dislocations. The 1-μm-thick [001] epilayer is rotated by an angle δ with respect to the 19-μm-thick [001] substrate. The average transmitted proton energy was measured as a function of tilt angle of the beam from the substrate [001] axis in the $(1\bar{1}0)$ planes.

binary collision approach in which small-angle approximations have been eliminated.[20] The energy loss and multiple scattering due to interactions with electrons is divided into contributions from inner-shell and valence electrons. The latter is simply approximated by a constant rate of energy loss dE/dz. The inner-shell electrons contribute an impact-parameter-dependent energy loss $\Delta E(b_i)$ at each collision. The dependence of the transmitted energy on the channeling conditions, which is vital to the current analysis, is therefore due to his contribution. The function $\Delta E(b_i)$ was calculated with the model of Dettmann and Robinson[21] as previously described.[18]

The system used in these simulations was a 1-μm-thick Si epilayer on a 19-μm Si substrate. These layer thicknesses are very close to those used in the experiments to be described in Sec. IV. The influence of the fraction of Ge on the epilayer was ignored. Since the critical angle for both planar and axial channeling scales with $\sqrt{Z_2}$, the error in the critical angles thus introduced is 3% and 9%, respectively, for the two SiGe compositions of 5% and 15% Ge to be described in Sec. IV. These small differences do not affect the general trends of the dechanneling effects of the 60° dislocations.

For all the simulated results in this section and the experimental results in Sec. IV, the bilayer sample is tilted away from the substrate [001] axis, in the $(1\bar{1}0)$ planes, such that channeling in the (110) planes only is altered. The channeling results are thus a combination of axial-to-planar channeling. The statistical noise level on the simulated results was 1 keV for each value of the simulated average proton energy at each tilt angle and rotation angle.

A. Simulated results

Figure 3 shows the average transmitted proton energy as a function of tilt angle of the beam from the substrate [001] axis in the $(1\bar{1}0)$ planes for different positive rotation angles of the epilayer. Symmetry considerations show that the effect of a layer rotated by $-\delta$ at a tilt angle $-\theta$ is the same as a positive rotation angle $+\delta$ at $+\theta$ and also that a tilt about the $(1\bar{1}0)$ planes produces a similar effect as about the (110) planes described here. A high transmitted energy corresponds to many ions being well channeled through the crystal and so losing energy at a low average rate, whereas a low transmitted energy corresponds to many ions being poorly channeled through the crystal and so losing energy at a high average rate. The case where $\delta=0.0°$ corresponds to a perfect crystal, and the resultant transmitted energy varies symmetrically about the maximum which occurs at $\theta=0.0°$, i.e., substrate [001] axial alignment. The tilt angles at which the average transmitted proton energy is lowest correspond to a blocking alignment,[22] where the protons are incident at an angle which is just large enough such that those entering near the center of the channels formed by the (110) planes can surmount the potential barrier of the planes bounding the channel. These protons then have lost almost all of their transverse kinetic energy when they reach the planes and therefore

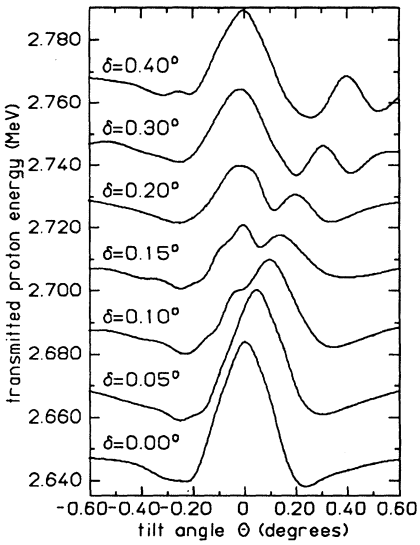

FIG. 3. Simulated values of the average energy of 3-MeV protons transmitted through a 1-μm Si layer and a 19-μm-thick substrate, as a function of tilt angle of the beam from the substrate [001] axis, in the $(1\bar{1}0)$ planes. The 1-μm-thick epilayer is at fixed rotation angle δ with respect to the substrate. Each curve is offset vertically by an additional 20 keV after the lowest curve for clarity.

travel a relatively long time close to the planes, resulting in a higher than average rate of energy loss. In the nuclear interaction probability as a function of incident angle, this effect shows up as a "shoulder" in the yield.

It is known[22] that the location of shoulders on an axial channel is determined by the shoulders of the planar channels passing through them, rather than by any simple features of the rows themselves. Therefore in the following we relate the features of the transmitted energy versus tilt angle and rotation angle to the critical angle for planar channeling, $\psi_c = 0.14°$, for 3-MeV protons.

There are essentially three regimes with differing magnitudes of the rotation angle of the epilayer which describe the shape of the resultant transmitted proton energy curve. For a small rotation $\delta \leq \psi_c/2$ (i.e., $\delta = 0.05°$ in Fig. 3), the resultant transmitted proton energy curve maintains the same symmetrical shape as for $\delta = 0.0°$, but is displaced along the horizontal axis away from substrate alignment by an amount $\theta = \delta$. For a large rotation, $\delta > 2\psi_c$ (i.e., $\delta = 0.3°, 0.4°$ in Fig. 3), there are two separate peaks in the transmitted proton energy curve. The large peak centered at $\theta = 0.0°$ is due to ions passing through the rotated epilayer with a nonchanneled rate of energy loss, but remaining reasonably collimated through this layer, and then channeling in the aligned substrate. The smaller peak centered at $\theta = \delta$ occurs when the sample is tilted such that the protons are channeled through the rotated epilayer, but pass through the misaligned substrate with a nonchanneled rate of energy loss. Intermediate tilt angles between these two peaks correspond to the incident ions being misaligned with both the epilayer and substrate and so do not channel well in either. For an intermediate rotation angle $\psi_c/2 < \delta < 2\psi_c$ (i.e., $\delta = 0.10°, 0.15°, 0.20°$ in Fig. 3), there is a more complex distribution of transmitted proton energy as a function of tilt angle as a result of the superposition of the separate effects of channeling in the substrate and channeling in the epilayer. As δ increases from 0.10°, the single transmitted energy peak splits into two separate peaks. At $\delta = 0.10°$ the maximum transmitted proton energy still occurs at a tilt angle of $\theta = \delta$, whereas for a larger rotation angle it occurs at a tilt angle of θ closer to 0.0°. It is predicted from these curves for the transmitted proton energy in Fig. 3 that for a small plane rotation angle of $\delta < 0.7\psi_c$ the maximum transmitted energy occurs at $\theta = \delta$, and so if the tilt angle for the maximum transmitted energy is measured at the dislocations, then the plane rotation angle across the 60° dislocations can be found. This is experimentally investigated in Sec. IV A.

Dislocations are visible in experimental transmission ion channeling images because the average transmitted proton energy at them is different compared with the surrounding perfect crystal. Their image "contrast" makes them appear as bright or dark regions in a grey scale image, showing the variation of the average transmitted proton energy.[12–14] Figure 4(a) shows the calculated dislocation contrast as a function of tilt angle of the beam from the substrate [001] axis in the $(1\bar{1}0)$ planes for the same positive rotation angles shown in Fig. 3. These curves were constructed by substracting the average transmitted proton energy for a particular rotation angle away from the transmitted energy for $\delta = 0.0°$ at the same tilt angle. A positive contrast value corresponds to the average transmitted proton energy being higher away from the dislocation at that tilt angle, and conversely a negative value corresponds to the average proton energy being greater at the dislocation for that tilt angle. For each rotation angle δ, there is an interval of θ values where the contrast is positive as well as an interval of negative contrast. It is predicted from Fig. 4(a) that a bunch of 60° dislocations will appear as a region with positive contrast at some tilt angle and negative contrast at some different tilt angle. The strongest contrast does not occur at exact planar or axial alignment, as has been previously thought, and this is also experimentally investigated in Sec. IV A.

Figure 4(b) shows curves for the maximum positive and negative dislocation contrast as a function of positive rotation angle, based on Fig. 4(a). The maximum positive and negative dislocation contrast occurs for $0.7\psi_c < \delta < 1.4\psi_c$ [i.e., between $\delta = 0.1°$ and 0.2° in Fig. 4(b)]. This is an important point as it shows, first, that care is needed to correctly interpret the observed image contrast. Second, it shows that for a given rotation angle of the 60° dislocations in a bunch, the beam type and energy can be tailored to give the strongest dislocation contrast, as changing these parameters changes the critical angle.

The tilt angles under which two adjacent bunches of 60° dislocations with slightly differing rotation angles can be individually resolved are now considered. Figure 5(a) shows the average transmitted proton energy as a function of rotation angle for fixed positive and negative tilt

angles away from the substrate [001] axis in the $(1\bar{1}0)$ planes. Consider two adjacent bunches of dislocations with rotation angles $\delta = +0.10°$ and $+0.05°$, which are shown by the vertically running dashed lines in Fig. 5(a) at different tilt angles. At large negative and positive tilt angles $\theta > 1.4\psi_c$ [i.e., $\theta > \pm 0.2°$ in Fig. 5(a)], there is no difference in the average transmitted proton energy from these two values of rotation angle, and so they cannot be individually resolved. For smaller tilt angles, there is a significant difference in the transmitted proton energy for these two values of rotation angle, and so they can be resolved. For a positive tilt angle, those protons

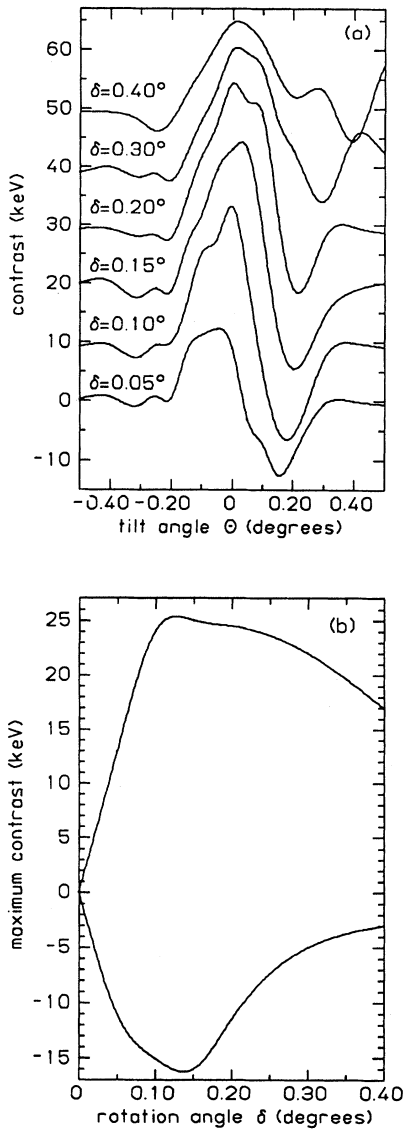

FIG. 4. (a) Simulated contrast from a 60° dislocation where the planes are rotated by a fixed angle δ. The contrast is shown as a function of tilt angle θ away from the substrate [001] axis about the (110) planes, with the beam still channeled in the $(1\bar{1}0)$ planes, relative to a perfect crystal (i.e., $\delta = 0.0°$). Positive and negative values mean that the average energy is, respectively, lower and higher at the dislocation than the perfect crystal. Each curve is offset vertically by an additional 10 keV after the lowest curve. (b) Maximum positive and negative dislocation contrast for 3-MeV protons as a function of rotation angle δ. These values were chosen from the maxima and minima of the humps and dips in (a) for any tilt angle.

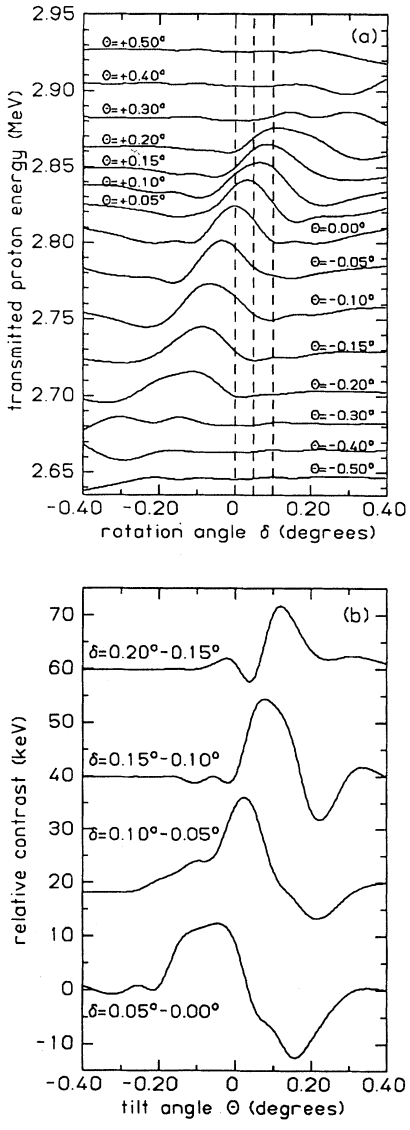

FIG. 5. (a) Simulated average transmitted proton energy for a fixed tilt angle θ of the beam from the substrate [001] axis in the $(1\bar{1}0)$ planes, as a function of rotation angle δ of the epilayer. Each curve is offset vertically by an additional 20 keV after the lowest curve. Vertically running dashed lines are shown at $\delta = 0.0°, 0.05°, 0.10°$ in order to indicate the relative values of transmitted energy for different tilt angles at these rotation angles. (b) Relative contrast between two adjacent bunches of 60° dislocations with rotation angles differing by 0.05°, as a function of tilt angle of the beam from the substrate [001] axis, in the $(1\bar{1}0)$ planes. The actual values of the rotation angles used are shown by each curve, which are offset vertically after the lowest curve for clarity.

transmitted through the bunch rotated through $\delta=0.10°$ have a lower transmitted energy than those transmitted through the bunch rotated through $\delta=0.05°$ and higher transmitted energy at a negative tilt angle. It is predicted from Fig. 5(a) that two adjacent bunches of 60° dislocations with planes rotated by slightly differing amounts can only be resolved from each other for a narrow range of tilt angles, which is experimentally investigated in Sec. IV B.

This consideration is important in interpreting the observed contrast in transmission ion channeled images. It is further highlighted in Fig. 5(b), which shows the difference in transmitted proton energy (i.e., relative contrast) as a function of tilt angle of the beam from the substrate [001] axis in the $(1\bar{1}0)$ planes for two 60° dislocation bunches producing two rotation angles which differ by 0.05°; the actual values are shown in Fig. 5(b). While a tilt angle of $\theta=-0.05°$ maximizes the positive contrast between bunches of dislocations with $\delta=0.05°$ and 0.0°, there is essentially no contrast between bunches of dislocations with $\delta=0.15°$ and 0.10° at this tilt angle. Conversely, where the positive contrast between the two bunches of dislocations with $\delta=0.15°$ and 0.10° is a maximum at a tilt angle of $\theta=0.10°$, the contrast is now negative from the two bunches of dislocations with $\delta=0.05°$ and 0.0°. As a general conclusion from Fig. 5(b), the larger the average rotation angle of two bunches of dislocations with slightly differing plane rotation angles, a larger tilt angle away from the substrate [001] axis is required to obtain the maximum contrast between them.

IV. COMPARISON WITH EXPERIMENTAL RESULTS

The predictions made using the simulated results in Sec. III for the average energy of protons transmitted through the rotated planes around 60° dislocations and the thinned substrate are now tested using our previously reported experimental results for two epitaxial $Si_{1-x}Ge_x/Si$ materials. Full details of the experimental procedure are given in Refs. 12 and 13 and are not repeated here. The first material is $Si_{0.95}Ge_{0.05}/Si$, which has a low dislocation density and is used to confirm that rotated planes due to the insertion of the $(a/2)[001]$ edge component of 60° dislocations are the major dechanneling mechanism and to show quantitative agreement on the magnitude of the change in transmitted proton energy across a spatially resolved group of five 60° misfit dislocations. The second material is $Si_{0.85}Ge_{0.15}/Si$, which has a higher 60° dislocation density and is used to investigate the prediction that adjacent bunches of 60° dislocations with planes rotated through slightly different amounts can only be resolved at specific tilt angles. For both materials the silicon substrate was mechanically thinned to 20 μm and then polished to remove any scratches larger than 1 μm, and a highly collimated MeV proton beam was focused to a spot size of 200 nm on sample surface for analysis.

A. $Si_{0.95}Ge_{0.05}/Si$ sample

This material consisted of a blank [001] Si substrate over which a 1.8-μm-thick $Si_{0.95}Ge_{0.05}$ layer was deposited by molecular beam epitaxy. This layer thickness is below the critical thickness at which dislocations were expected to be generated to relieve the strain, but there were a few dislocations present in localized regions,[23] and they run out along the [110] and $[1\bar{1}0]$ directions to form a "cross".[24] The number of dislocations present in each of the cross arms decreased with increasing distance away from the center, and the number of dislocations present was determined by independent methods as described in Ref. 13. Since the epilayer thickness was 1.8 μm, a small discrepancy between the measured and simulated values was expected here as the simulated results described in Sec. III assume an epilayer thickness of 1 μm.

Experimental transmission-ion-channeled images were measured from this material with 3-MeV protons.[13] The beam was channeled in the substrate [001] axis, and the sample was tilted in 0.10° steps with respect to the (110) planes with the beam still channeled in the $(1\bar{1}0)$ planes. The measured value of $\psi_{1/2}$ is $0.12°\pm0.01°$, compared with the channeling critical angle of $\psi_c=0.14°$. Figure 6(a) shows measured line scans in histogram form for the average transmitted proton energy as a function of distance across a bunch of five 60° dislocations of this cross for different tilt angles. The variation of the average transmitted proton energy is plotted relative to the level measured from the surrounding perfect crystal, which is shown as 0 keV for each tilt angle. At a large negative tilt angle, the protons have a higher transmitted energy at the dislocations than the surrounding perfect crystal. At a tilt angle of between $\theta=-0.13°$ and $-0.03°$, the contrast changes sign such that the average transmitted proton energy is lower at the dislocations than the surrounding perfect crystal. With increasing positive tilt angle, the difference in the transmitted energy at the dislocation compared with the surrounding perfect crystal gradually decreases until at $\theta=+0.27°$ the dislocations cannot be resolved from the surrounding crystal.

These measured line scans for the average transmitted proton energy were used to construct a single line scan showing the tilt angle at which the maximum transmitted proton energy occurred across this same area,[25] as shown in Fig. 6(b). The measured tilt angle across this area for maximum transmitted proton energy increases toward the middle of the bunch of five dislocations in the same sense on both sides up to a maximum of $\theta=-0.031°$. It was predicted from Fig. 3 that for a small rotation angle of $\delta<0.7\psi_c$ the tilt angle at which the transmitted proton energy was a maximum occurred at the rotation angle of the epilayer. Since in Fig. 6(b) the value of the tilt angle across the dislocations bunch for maximum transmitted energy is at most $\sim0.2\psi_c$, it is considered to be a direct measure of the spatial variation of the rotation angle across this group of five 60° dislocations.

If this interpretation is correct, then the curve given in Fig. 6(b) determines, with the help of the simulated results described in Sec. III, the average transmitted proton energy for any tilt angle for all positions along the line scan. Figure 6(a) shows these predicted curves as the solid lines superposed on the experimental results, where they are also plotted relative to the transmitted energy for a perfect crystal at that tilt angle. At a tilt angle of

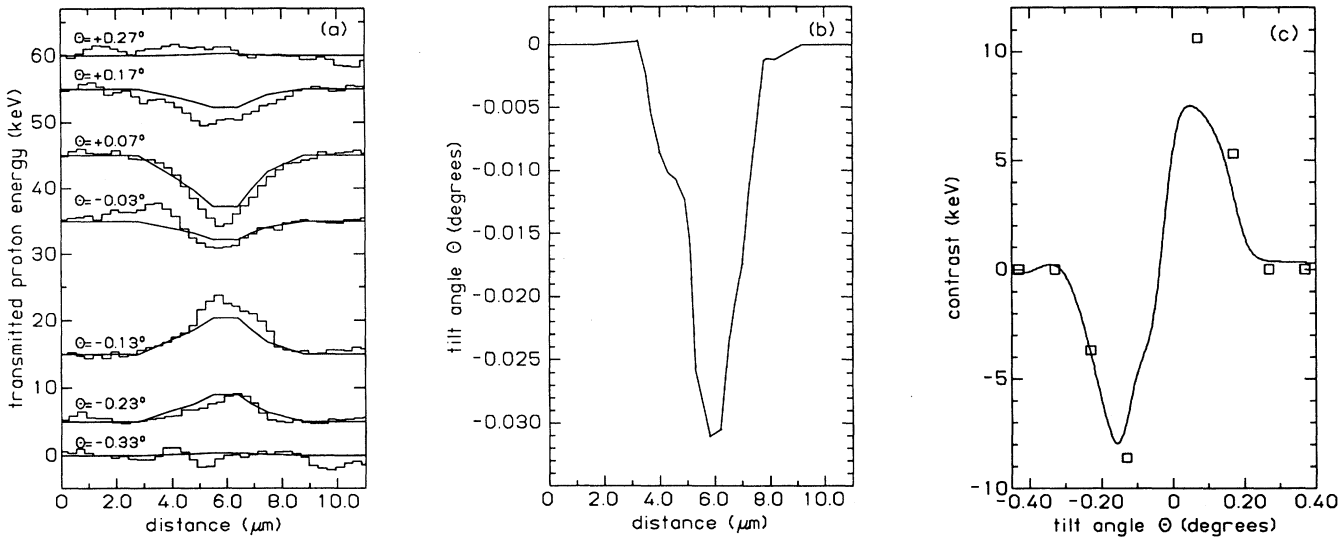

FIG. 6. (a) Experimental and simulated line scans extracted from across a region of five 60° dislocations. The curves show the average transmitted proton energy above the background level, shown as 0 keV, from the surrounding perfect crystal as a function of tilt angle of the beam from the substrate [001] axis in the $(1\bar{1}0)$ planes. The experimental data are represented by a histogram plot and the simulated data are shown as solid lines. Each curve is offset vertically for clarity. (b) Tilt angles θ for the maximum average transmitted proton energy across the five dislocations. This tilt angle is considered to be a measure of the spatial variation of the rotation angle across this region. (c) Maximum measured contrast from the group of five 60° dislocations as a function of tilt angle, shown as the data points. The maximum simulated contrast is also shown as the solid line, based on a rotation angle of $-0.031°$.

$\theta=-0.33°$, the simulated and experimental results show no difference in transmitted energy. At $\theta=-0.23°$ and $-0.13°$, there is increasingly higher transmitted proton energy at the dislocations due to protons channeling better here than in the perfect crystal. By $\theta=-0.03°$ the opposite occurs in both the simulated and experimental results. Since the simulated results are in good agreement with the measured change of transmitted proton energy as a function of tilt angle shown in Fig. 6(a), we conclude, first, that the major dechanneling mechanism from 60° dislocations is the resultant rotation of the epilayer due to the $(a/2)[001]$ component and, second, that these simulations are able to give good predictions of the variation of the observed transmission channeled image contrast from 60° dislocations.

There is a small discrepancy between the behavior of the experimental simulated line scans at the left-hand side for a tilt angle $\theta=-0.03°$ where the experimental transmitted proton energy is higher than the surrounding material, and this does not appear in the simulated curve. This may be due to the additional $(a/4)[1\bar{1}0]$ component of the 60° dislocations which was not incorporated into the dechanneling model described in Sec. III. This constitutes the limiting factor in considering the dechanneling effect from 60° dislocations to be due solely to inclined planes due to the $(a/2)[001]$ component.

Figure 6(c) shows the maximum measured contrast from the group of five 60° dislocations as a function of tilt angle, based on the line scans shown in Fig. 6(a). The maximum simulated contrast is also shown, based on a rotation angle of $\delta=-0.031°$ of the epilayer with respect to the substrate. There is good agreement between the tilt angle at which maximum positive and negative contrast occurs and also in the variation of the contrast as a function of tilt angle. This confirms that the curves shown in Fig. 4 correctly predict that the strongest contrast does not occur at perfect channeling alignment and that they give a good prediction of the variation of the contrast as a function of tilt angle. The magnitude of the positive contrast shown in Fig. 6(c) is 11 keV, compared with a simulated value of 8 keV. This discrepancy is probably due to the difference in the epilayer thickness of 1.8 μm in the measured results compared with the simulated results which used a value of 1 μm.

From Fig. 6 a plane rotation angle of $\delta=-0.031°$ results in a maximum difference of 11 keV to the average transmitted proton energy, above the experimental noise level of ± 1 keV. According to this, the minimum plane rotation which is just resolvable from the noise level is about 0.003° under presently attainable experimental conditions. This is better than previously reported sensitivity limits for dechanneling due to inclined planes in strain measurements using ion channeling, which are in the range of 0.01°–0.03°.[4] The difference arises mainly through the use of MeV protons for this transmission work, which have a narrower critical angle than MeV α particles (the ions commonly used for strain measurements as they enable depth-resolved information to be obtained).

B. $Si_{0.85}Ge_{0.15}$/Si sample

A $Si_{0.85}Ge_{0.15}$/Si sample which had a higher dislocation density than the sample considered above was used

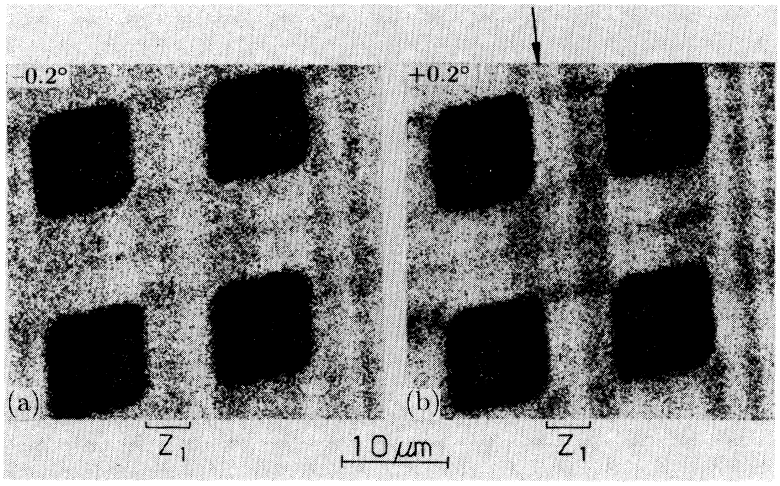

FIG. 7. Two 40×40 μm^2 transmission-ion-channeled images of a region containing four 10×10 μm^2 mesas (Ref. 12). The sample was tilted about the vertical axis, away from the substrate [001] axis with the beam channeled in the $(1\bar{1}0)$ planes to (a) $\theta=-0.2°$ and (b) $\theta=+0.2°$. Dark regions mean lower transmitted proton energy, equivalent to positive contrast, and bright regions mean higher transmitted proton energy, equivalent to negative contrast.

to investigate the predictions made using Fig. 5 that adjacent bunches of 60° dislocations with slightly differing rotation angles δ could only be resolved at certain tilt angles. The [001] substrate had been patterned to produce 3-μm-high raised mesas of varying lateral sizes, and a 1-μm-thick $Si_{0.85}Ge_{0.15}$ layer was deposited by molecular beam epitaxy. Transmission electron microscopy results showed that the 60° dislocations present occurred in bunches,[12] in which the average dislocation spacing varied from 50 to 300 nm. The edge component of these 60° dislocations has a Burgers vector $b=0.27$ nm, and so for $l=50$ nm (bunched dislocations), $\delta=0.31°$, while for $l=300$ nm (widely spaced dislocations), $\delta=0.05°$. On tilting from [001] axial channeling to $(1\bar{1}0)$ planar channeling, the measured value of $\psi_{1/2}$ was $0.21°\pm0.02°$ (Ref. 12) compared with the channeling critical angle for 2-MeV protons of $\psi_c=0.17°$. It was assumed that the behavior of the simulated curves for 2-MeV protons would be the same as for 3-MeV protons except that the magnitude of both δ and θ in Figs. 3–5 must be scaled by the ratio of the critical angles, i.e., by $(0.17/0.14)\sim1.2$. This discussion does not consider the small difference in the magnitude of the contrast for 2-MeV protons compared with 3-MeV protons due to their higher rate of energy loss since we are considering here the tilt angles at which the contrast changes and not the magnitude of the contrast.

Figure 7 shows two 40×40 μm^2 transmission-ion-channeled images of the same region of the 20-μm-thick $Si_{0.85}Ge_{0.15}$/Si sample at tilt angles of (a) $\theta=-0.2°$ and (b) $\theta=+0.2°$ away from the substrate [001] axis in the $(1\bar{1}0)$ planes. Dark regions represent a low average transmitted proton energy and light regions represent a high average transmitted proton energy. The four dark square regions are 10×10 μm^2 mesas, which are not discussed here, and zones of dislocations can be seen between the mesas as alternating bright and dark regions of contrast. Figure 8 shows a schematic of the rotated planes within different zones of 60° dislocations in this material, which was used to explain the observed contrast.[12] Different bunches of dislocations, labeled (b), present within each of these zones have slightly different rotation angles, but are of the same sign. Consider the variation of contrast from bunches of dislocations within zone Z_1 in Fig. 7, which is about 4 μm wide. There is uniformly dark contrast from this zone at $\theta=-0.2°$ (i.e., a tilt angle of approximately $-\psi_c$), whereas at $\theta=+0.2°$ (i.e., a tilt angle of approximately $+\psi_c$) there is mainly bright contrast from this region except for a narrow faint 1-μm-wide dark band, which is arrowed and cannot be seen at $\theta=-0.2°$.

As in Sec. IV A, by combining a series of transmitted proton energy images of this same area measured at slightly different tilt angles, the rotation angle of the bunches of 60° dislocations within this zone was found to vary between $+0.02°$ at the 1-μm-wide band to $+0.06°$ in the surrounding region within this zone.[25] The change of contrast in zone Z_1 at the different tilt angles can now be explained using Fig. 5(a). Consider two bunches of dislocations in Fig. 5(a) with $\delta=0.05°$ and $0.0°$, which gives a guide to the situation considered in Fig. 7 for rotation angles of $+0.06°$ and $+0.02°$ for 2-MeV protons. At a tilt angle of $\theta=-\psi_c$ in Fig. 5(a), there is no difference in transmitted proton energy from these two bunches of dislocations with $\delta=0.0°,0.05°$, and so the two dislocation bunches with $\delta=0.02°,0.06°$ cannot be resolved in Fig. 7(a). At a tilt of $\theta=+\psi_c$ in Fig. 5(a), there is significant difference in transmitted proton energy from

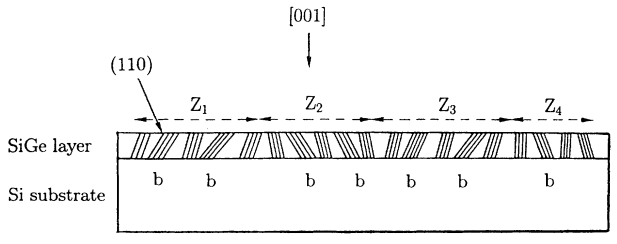

FIG. 8. Schematic showing the rotated planes in the bunches labeled (b) of 60° dislocations which are responsible for the observed contrast in Fig. 7. The dislocation bunches within zones Z_1 and Z_3 are bent in the opposite sense compared with zones Z_2 and zones Z_4, and so the sign of the plane rotation angle δ is opposite.

the two bunches of dislocations with $\delta=0.0°, 0.05°$, and so the two bunches with $\delta=0.02°, 0.06°$ can be resolved in Fig. 7(b). The bunch rotated through $\delta=0.0°$ gives a lower transmitted proton energy than the bunch rotated through $\delta=0.05°$ at $\theta=+\psi_c$, according to Fig. 5(a), and so the bunch rotated through $\delta=0.02°$ consequently appears darker in Fig. 7(b) compared with the surrounding bunches rotated through $\delta=0.06°$. It is concluded from this that the simulated results for the average transmitted proton energy correctly predict the tilt angles at which 60° dislocation bunches can and cannot be individually resolved from surrounding bunches.

V. CONCLUSIONS

A model for dechanneling from 60° dislocations due to the $(a/2)[001]$ component has been described. A Monte Carlo channeling program has been used to simulate the average transmitted energy of 3-MeV protons through a rotated epilayer and a thin substrate and the conditions under which 60° dislocations can be resolved from the surrounding perfect crystal and also from adjacent 60° dislocation bunches with planes rotated by slightly differing amounts. Two $Si_{1-x}Ge_x/Si$ materials have been used to experimentally investigate these simulated results, and good agreement was shown across a spatially resolved bunch of five 60° misfit dislocations and also from bunches of dislocations rotated through slightly differing amounts.

The position dependence of the electronic stopping was modeled in this work by the Dettmann-Robinson[21] theory, applied to the core electrons. More sophisticated models have been recently developed for the core-electron effects.[26,27] Also, recent experiments and calculations indicate that the effect of the spatial variation of the valence-electron density may not be neglected.[28] The results of the present analysis might change somewhat if more accurate models were used for the energy loss due to core electrons as well as valence electrons and we intend to study such effects. However, the trajectory of an ion depends only slightly on the energy loss model used. In other words, the fraction of channeled trajectories at various tilt angles θ and rotation angles δ of the epilayer will not change significantly. Thus the general features of Fig. 4 are unlikely to be affected, although the values of the average energies and the amplitude of the structures may vary.

There are two main limitations of using this model to measure variations in the average transmitted proton energy through epitaxial layers due to dechanneling from rotated planes due to the $(a/2)[001]$ component. First, the effect of the $(a/4)[1\bar{1}0]$ component on dechanneling has not been incorporated and there was some evidence in Fig. 6(a) that this effect may be significant. Second, the variation of the rotation angle of the planes through the thickness of the epitaxial layer at a fixed lateral distance away from the dislocation bunch has not been considered here. These two factors will be investigated in order to further improve this model.

ACKNOWLEDGMENT

P.J.C.K. wishes to thank the Royal Commission for the Exhibition of 1851 for financial support to pursue this work.

[1] J. C. Bean, J. Vac. Sci. Technol. B **4**,(6) 1427 (1986).
[2] J. W. Matthews and A. E. Blakeslee, J. Cryst. Growth **27**, 118 (1974).
[3] L. C. Feldman, J. W. Mayer, and S. T. Picraux, *Materials Analysis by Ion Channeling* (Academic, New York, 1982).
[4] S. T. Picraux, B. L. Doyle, and J. Y. Tsao, Semicond. Semimet. **33**, 139 (1991).
[5] S. T. Picraux, L. R. Dawson, G. C. Osbourn, and W. K. Chu, Appl. Phys. Lett. **43**, 930 (1983).
[6] S. T. Picraux, W. R. Allen, R. M. Biefeld, J. A. Ellison, and W. K. Chu, Phys. Rev. Lett. **54**, 2355 (1985).
[7] J. H. Barrett, Phys. Rev. B **28**, 2328 (1983).
[8] S. T. Picraux, L. R. Dawson, J. Y. Tsao, B. L. Doyle, and S. R. Lee, Nucl. Instrum. Methods B **33**, 891 (1988).
[9] A. C. Chami, E. Ligeon, R. Danielou, J. Fontenille, G. Lentz, N. Magnea, and H. Mariette, Appl. Phys. Lett. **52**, 1874 (1988).
[10] Y. Quéré, Phys. Status Solidi **30**, 713 (1968).
[11] F. Romanato, M. Mazzer, and A. V. Drigo, Nucl. Instrum. Methods B **63**, 36 (1992).
[12] M. B. H. Breese, P. J. C. King, J. Whitehurst, G. R. Booker, G. W. Grime, F. Watt, L. T. Romano, and E. H. C. Parker, J. Appl. Phys. **73**, 2640 (1993).
[13] P. J. C. King, M. B. H. Breese, G. R. Booker, P. R. Wilshaw, J. Whitehurst, G. W. Grime, F. Watt, and M. J. Goringe, Nucl. Instrum. Methods B **77**, 320 (1993).
[14] P. J. C. King, M. B. H. Breese, P. R. Wilshaw, G. R. Booker, G. W. Grime, F. Watt, and M. J. Goringe, in *Microscopy of Semiconducting Materials 1993,* Proceedings of Royal Microscopical Society Conference, Oxford, edited by A. G. Cullis, A. E. Staton-Bevan, and J. L. Hutchinson, IOP Conf. Proc. No. 134 (Institute of Physics and Physical Society, London, 1993), p. 153.
[15] G. W. Grime, M. Dawson, M. Marsh, I. C. McArthur, and F. Watt, Nucl. Instrum. Methods B **54**, 52 (1991).
[16] *Channeling Theory, Observations and Applications,* edited by D. V. Morgan (Wiley, New York, 1973).
[17] L. C. Feldman and B. R. Appleton, Phys. Rev. **8**, 935 (1973).
[18] P. J. M. Smulders and D. O. Boerma, Nucl. Instrum. Methods B **29**, 471 (1987).
[19] P. J. M. Smulders, D. O. Boerma, and M. Shaanan, Nucl. Instrum. Methods B **45**, 450 (1990).
[20] A. Dygo,W. N. Lennard, I. V. Mitchell, and P. J. M. Smulders, Nucl. Instrum. Methods B **90**, 161 (1994).
[21] K. Dettmann and M. T. Robinson, Phys. Rev. B **10**, 1 (1974).
[22] J. H. Barrett, Phys. Rev. **166**, 219 (1968).
[23] C. G. Tuppen, C. J. Gibbings, and M. Hockly, J. Cryst. Growth **94**, 392 (1989).
[24] C. J. Gibbings, C. G. Tuppen, and M. Hockley, Appl. Phys. Lett. **54**, 148 (1989).
[25] P. J. C. King, Ph.D. thesis, University of Oxford, 1993.
[26] E. H. Mortensen, H. H. Mikkelsen, and P. Sigmund, Nucl. Instum. Methods B **61**, 139 (1991).
[27] N. M. Kabachnik, V. N. Kondratev, and O. V. Chumanova, Phys. Status Solidi B **145**, 103 (1988).
[28] A. Dygo, M. A. Boshart, L. E. Seiberling, and N. M. Kabachnik, Phys. Rev. A **50**, 4979 (1994).

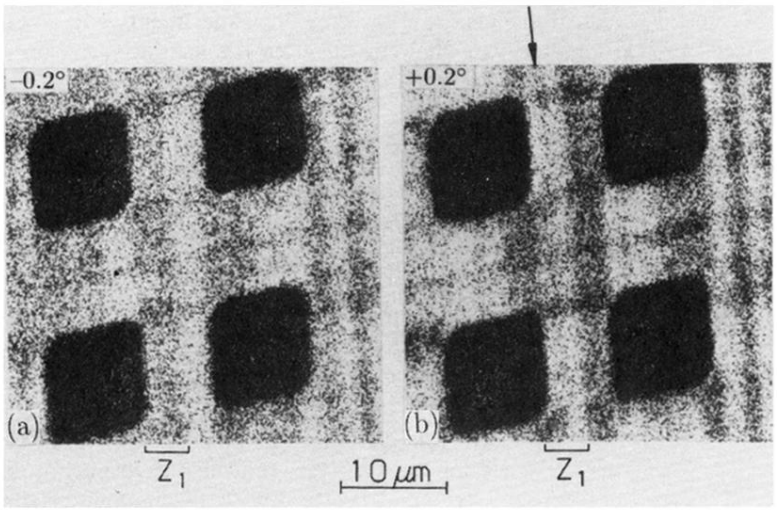

FIG. 7. Two 40×40 μm^2 transmission-ion-channeled images of a region containing four 10×10 μm^2 mesas (Ref. 12). The sample was tilted about the vertical axis, away from the substrate [001] axis with the beam channeled in the $(1\bar{1}0)$ planes to (a) $\theta=-0.2°$ and (b) $\theta=+0.2°$. Dark regions mean lower transmitted proton energy, equivalent to positive contrast, and bright regions mean higher transmitted proton energy, equivalent to negative contrast.